3100-2890, 2830, 1691 (s, br), 1611, 1513 (s), 1470-1435, 1415, 1385, 1280, 1250, 1182 (s, br), 1113, 1040, 1000, 918, 828 (s) cm^{-1}. ^1H NMR ($CDCl_3$, 360 MHz): 7.21 (m, 2 H), 7.07 (dd, 1 H, J = 10.29, 1.06 Hz), 6.88 (m, 2 H), 6.16 (dd, 1 H, J = 10.27, 0.62 Hz), 5.61-5.49 (m, 1 H), 5.09 (dm, 1 H, J = 17.44 Hz), 5.07 (dm, 1 H, J = 9.81 Hz), 3.80 (s, 3 H), 2.68 (ddt, 1 H, J = 13.98, 5.95, 1.41 Hz), 2.47 (ddt, 1 H, J = 14.03, 8.44, 0.80 Hz), 2.36-2.18 (m, 4 H). ^{13}C NMR ($CDCl_3$, 50 MHz): 199.5, 158.3, 155.4, 134.8, 133.5, 129.3, 127.8, 118.8, 113.9, 55.3, 46.3, 43.2, 35.9, 34.4. Mass spectrum, calcd for $C_{16}H_{18}O_2$ 242.1307, found 242.1307. IR and ^1H NMR data show good agreement with literature values.

Acknowledgment. The authors gratefully acknowledge the financial support provided by the National Science Foundation (Grant No. CHE-8719728). We also thank the Midwest Regional Center of Mass Spectrometry at the University of Nebraska—Lincoln for technical assistance.

Dependence of Transition-State Structure on Acyl Chain Length for Cholesterol Esterase Catalyzed Hydrolysis of Lipid *p*-Nitrophenyl Esters

Larry D. Sutton,† Jay S. Stout, and Daniel M. Quinn*

Contribution from the Department of Chemistry, University of Iowa, Iowa City, Iowa 52242.
Received December 18, 1989

Abstract: Cholesterol esterase (CEase) catalyzes hydrolysis of lipid substrates via a serine esterase mechanism. A variety of reaction kinetic probes has been used to characterize features of the mechanistic anatomy of porcine pancreatic CEase-catalyzed hydrolysis of lipid *p*-nitrophenyl esters that have acyl chain lengths from C_2 to C_{12}. Nucleophilic trapping experiments demonstrate that k_{cat} is rate-limited by deacylation across the homologous series of substrates. The dependence of k_{cat}/K_m on acyl chain length displays a maximum for the C_6 ester. Both the ascending and descending limbs of the structure–reactivity profile give linear free energy plots of ln (k_{cat}/K_m) versus the number of acyl carbons of substrate, with slopes that yield $\Delta\Delta G^{\ddagger} = -430$ and 470 cal/mol per methylene, respectively. Solvent isotope effects ($^{D_2O}k_{cat}/K_m$) decrease from ~2 for short esters to ~1.2 for long esters. Except for the C_2 and C_3 esters, proton inventories of k_{cat}/K_m are linear. These results indicate that the phenomenological transition state for the acylation stage of CEase catalysis is highly variable: For short substrates (C_2 and C_3), serial microscopic transition states contribute to rate determination. For the C_4 substrate, a single transition state that is stabilized by a single general-acid–base proton transfer is rate-determining, while with increasing acyl chain length rate determination shifts between parallel reaction pathways. The deacylation rate constant k_{cat} is nearly invariant for C_4–C_8 substrates but drops off sharply for C_{10} and C_{12} substrates. However, solvent isotope effects ($^{D_2O}k_{cat}$) are ~2, and proton inventories are linear for all substrates. Therefore, both the acylation and deacylation stages of CEase-catalyzed hydrolysis of lipid *p*-nitrophenyl esters have chemical transition states that are stabilized by single proton transfers.

Introduction

Pancreatic cholesterol esterase (CEase[1]) is secreted into the duodenum in response to an oral fat load, where it catalyzes the hydrolysis of cholesteryl esters, phospholipids, and acylglycerols.[2-4] The enzyme is necessary for full absorption of dietary fats, including cholesterol, across the intestinal mucosa into the bloodstream.[5,6] Because of this physiological role and since CEase efficiently catalyzes the hydrolysis of structurally diverse substrates, studies of CEase catalysis are of great interest.

It is believed that CEase belongs to the serine hydrolase class of enzymes[7,8] whose reactions proceed via the acylenzyme mechanism depicted in Scheme I.[9] This mechanism involves nucleophilic attack by serine, aided by general-base catalysis by histidine, on the scissile carbonyl carbon of the substrate, eventually leading to the acylenzyme intermediate. Water attacks the acylenzyme, again aided by general-base catalysis by histidine. This mechanism has received powerful support from the recent report by Kissel et al.[10] of the primary sequence of rat pancreatic CEase, deduced from the corresponding cDNA sequence. The mature enzyme contains 592 amino acids, of which a 63 amino acid domain (residues 159-221) shows high similarity to the active-site regions of *Torpedo californica* acetylcholinesterase[11] and human serum butyrylcholinesterase.[12] In particular, the sequence that contains the active-site serines (starred) of the cholinesterases, V-T-I/L-F-G-E-S*-A-G-G/A-A-S-V, is nearly identical with the corresponding sequences that contains S194 in CEase. Despite the sequence information, many features of the chemical mechanism of CEase catalysis are undefined.

Scheme I. Cholesterol Esterase Mechanism

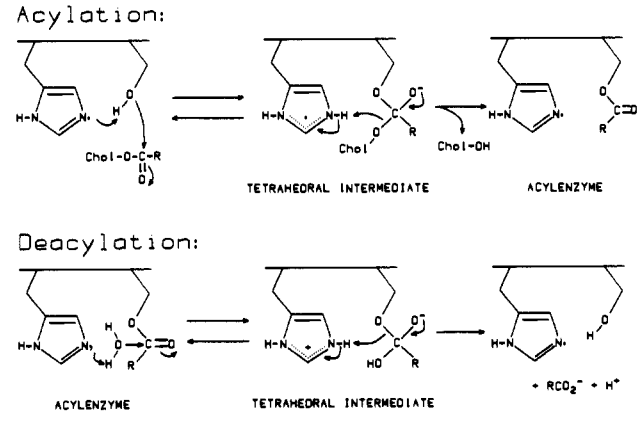

This study was designed to answer several questions concerning

* To whom correspondence should be addressed.

† Current address: Department of Pathology, University of Iowa Hospitals and Clinics, Iowa City, IA 52242.

(1) Abbreviations: CEase, cholesterol esterase; AChE, acetylcholinesterase; BuChE, butyrylcholinesterase; PNPA, *p*-nitrophenyl acetate, the C_2 ester; PNPP, *p*-nitrophenyl propanoate, the C_3 ester; PNPB, *p*-nitrophenyl butyrate, the C_4 ester; PNPV, *p*-nitrophenyl valerate, the C_5 ester; PNPC, *p*-nitrophenyl caproate, the C_6 ester; PNPO, *p*-nitrophenyl octanoate, the C_8 ester; PNPD, *p*-nitrophenyl decanoate, the C_{10} ester; PNPL, *p*-nitrophenyl laurate, the C_{12} ester; MeCN, acetonitrile; TX100, Triton X-100; LpL, lipoprotein lipase; $[S]_0$, initial substrate concentration; $[E]_T$, analytical enzyme concentration; V, maximal velocity, $V_{max} = k_{cat}[E]_T$; K, Michaelis constant, K_m; V/K, first-order rate constant when $[S]_0 \leq K/10$; k_{cat}/K, second-order acylation rate constant, sometimes called k_E; $^{D_2O}k_{cat}$ and $^{D_2O}k_{cat}/K$, observed solvent isotope effects for $k_{cat}(V)$ and $k_{cat}/K(V/K)$, respectively; SDS-PAGE, sodium dodecyl sulfate polyacrylamide gel electrophoresis; BCA, bicinchoninic acid.

0002-7863/90/1512-8398$02.50/0

CEase-catalyzed reactions: (a) What limits the rate for V (= $k_{cat}[E]_T$) of CEase-catalyzed reactions? (b) Does CEase stabilize chemical transition states via proton-transfer catalysis and, therefore, display sizable solvent deuterium isotope effects? (c) Does transition-state stabilization involve single proton transfer (simple general-acid–base) catalysis or multiple-proton-transfer (multifunctional) catalysis? The charge-relay mechanism of serine protease catalyzed hydrolysis of peptide substrates[13-17] provides an example of multiproton catalysis. (d) Does the structure of the transition state change as the structure of the substrate is systematically varied? These questions are addressed herein for CEase-catalyzed hydrolysis of a homologous series of lipid *p*-nitrophenyl esters whose fatty acyl chains range in length from C_2 to C_{12} by measuring solvent isotope effects, pH–rate effects, effects of structure on reactivity, and nucleophilic trapping experiments.

Experimental Section

Enzyme Purification. CEase (EC 3.1.1.13) was isolated from porcine pancreas that was purchased from a local slaughterhouse. Immediately upon removal from the animals, the pancreases were frozen on dry ice. The enzyme was purified by a modification of the procedure developed in Brockman's laboratory.[18-19] Isolation involved frozen pancreas homogenization, heat and ammonium sulfate precipitations, *tert*-butyl alcohol extraction, and Sephacryl S-200 and Sephadex G-100 column chromatographies. The preparation gave a single band on SDS-PAGE, and the concentration of enzyme fractions was determined by the BCA[20] assay. Molar enzyme concentrations were calculated with a molecular mass of 80 000. The enzyme was stored at −70 °C in 0.1 M sodium phosphate buffer, pH 7.0, that contained 0.1 N NaCl, 2 mM benzamidine hydrochloride, 3 mM sodium taurocholate, and 0.2 mM *N*-benzoyl-*d*,*l*-arginine.

Materials. Triton X-100; Sephadex G-100; and *p*-nitrophenyl esters of ethanoic, propanoic, butanoic, pentanoic, hexanoic, octanoic, decanoic, and dodecanoic acids were purchased from Sigma Chemical Co. Deuterium oxide (99.8% D) was purchased from Sigma and Aldrich. HPLC-grade acetonitrile was purchased from Fisher Scientific, Sephacryl S-200 from Pharmacia Fine Chemicals, and BCA protein assay reagent from Pierce Chemical Co. All salts used in buffer preparation were commercially available reagent-grade products. Protium oxide was distilled and deionized by passage through a Barnstead mixed-bed ion-exchange column (Sybron Corp.). Silica-coated plastic TLC slides were purchased from Macherey Nagel.

Scheme II. Nucleophilic Trapping of Acylenzyme

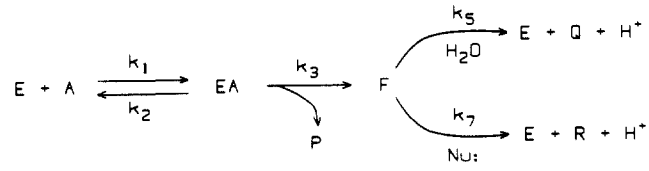

Nucleophilic Trapping Experiments. The laurylhydroxamate formed during CEase-catalyzed turnover of PNPL in the presence of NH_2OH was quantitated essentially as described by Burdette and Quinn[21] for LpL-catalyzed turnover of PNPL. Nucleophilic trapping experiments were conducted at 20 °C in 0.1 M sodium phosphate buffer, pH 7.10, that contained 0.1 N NaCl, 1.1 mM TX100, 38 μM PNPL, and the indicated concentrations (cf. Results) of NH_2OH and CEase. Controls contained all components save CEase.

Kinetic Measurements and Data Reduction. Reactions were followed by monitoring the formation of *p*-nitrophenoxide versus time on a Beckman DU40 UV–visible spectrophotometer or on a Zymate I robotics system[22] that is interfaced to a Beckman DU7 UV–visible spectrophotometer. Time courses were followed at 400 nm for reactions that contained ≤0.1 mM substrate and at 450 nm otherwise. Reaction temperatures were maintained at ±0.05 °C on the DU40 and at ±0.02 °C on the robotics system with use of Lauda RC3 and Grant LTD 6 refrigerated, circulating water baths, respectively. The pH values of buffers were measured with a Corning Model 125 pH meter that is equipped with a glass combination electrode. For buffers in D_2O, 0.4 was added to the pH meter reading.[23]

Equivalent buffers[24,25] in H_2O (pH 7.01 ± 0.03) and D_2O (pD 7.55 ± 0.02) were used for solvent isotope effect and proton inventory experiments. Mixed micelles of TX100 and *p*-nitrophenyl esters were prepared as described by Burdette and Quinn.[21] Solutions for the pH–rate profile experiments were made by injection of a small volume of the substrate in MeCN into buffer that contained TX100. Reactions were initiated by adding an aliquot of enzyme into the reaction solution. Components of reaction buffers are specified in table footnotes and figure legends.

Michaelis–Menten kinetic parameters were determined by nonlinear least-squares fitting[26] of time course data to the integrated form of the Michaelis–Menten equation.[9] A, A_0, and A_∞ are the absorbances at

$$t = \frac{K}{V}\ln\frac{A_\infty - A_0}{A_\infty - A} + \frac{A - A_0}{V(\epsilon_p - \epsilon_s)} \quad (1)$$

times t, 0, and ∞, respectively; ϵ_p and ϵ_s are the respective absorptivity constants of product and substrate. First-order rate constants (i.e., V/K) were also measured, when $[S]_0 < K/10$, by nonlinear least-squares fitting[26] of time course data to eq 2.

$$A = (A_0 - A_\infty)e^{-(V/K)t} + A_\infty \quad (2)$$

pH–rate profiles were determined by fitting reaction time courses at various pH values to eq 1. The bell-shaped pH–V profile was fit to eq 3. In eq 3, three protonic states of CEase are in equilibrium, but only

$$V^{obs} = \frac{V^{lim}}{1 + 10^{pK_{f1}-pH} + 10^{pH-pK_{f2}}} \quad (3)$$

the intermediate protonic state is catalytically competent. V^{obs} is the observed V, V^{lim} is the V of the active form, and pK_{f1} and pK_{f2} are the pK values of the active site amino acids on whose basic and acidic forms, respectively, activity depends. The pH–V/K profile is described in the Results.

Proton inventories consist of rate measurements in mixed buffers of H_2O and D_2O of atom fraction of deuterium n and are described by eq 4 when reactant state fractionation factors are unity.[24,25] Hence, a plot

$$k_n = k_0\prod_i^{X}(1 - n + n\phi^T_i) \quad (4)$$

of k_n versus n is linear if a single transition-state proton contributes to

(2) Brockerhoff, H.; Jensen, R. G. *Lipolytic Enzymes*; Academic Press: New York, 1974; pp 176–193.
(3) Kritchevsky, D.; Kothari, H. V. *Adv. Lipid Res.* **1978**, *16*, 221–226.
(4) Rudd, E. A.; Brockman, H. L. In *Lipases*; Borgström, B., Brockman, H. L., Eds.: Elsevier: Amsterdam, 1984; pp 185–204.
(5) Bhat, S. G.; Brockman, H. L. *Biochem. Biophys. Res. Commun.* **1982**, *109*, 486–492.
(6) Gallo, L. L.; Clark, S. B.; Myers, S.; Vahouny, G. V. *J. Lipid Res.* **1985**, *25*, 604–612.
(7) Blow, D. M. *Acc. Chem. Res.* **1976**, *9*, 145–152.
(8) Stroud, R. M. *Sci. Am.* **1974**, *231*, 74–88.
(9) Stout, J. S.; Sutton, L. D.; Quinn, D. M. *Biochim. Biophys. Acta* **1985**, *837*, 6–12.
(10) Kissel, J. A.; Fontaine, R. N.; Turck, C. W.; Brockman, H. L.; Hui, D. Y. *Biochim. Biophys. Acta* **1989**, *1006*, 227–236.
(11) Schumacher, M.; Camp, S.; Maulet, Y.; Newton, M.; MacPhee-Quigley, K.; Taylor, S. S.; Friedmann. T.; Taylor, P. *Nature* **1986**, *319*, 407–409.
(12) Lockridge, O.; Bartels, C. F.; Vaughan, T. A.; Wong, C. K.; Norton, S. E.; Johnson, L. L. *J. Biol. Chem.* **1987**, *262*, 549–557.
(13) Hunkapiller, M. W.; Forgac, M. D.; Richards, J. H. *Biochemistry* **1976**, *15*, 5581–5588.
(14) Elrod, J. P.; Hogg, J. L.; Quinn, D. M.; Venkatasubban, K. S.; Schowen, R. L. *J. Am. Chem. Soc.* **1980**, *102*, 3917–3922.
(15) Stein. R. L.; Elrod, J. P.; Schowen, R. L. *J. Am. Chem. Soc.* **1983**, *105*, 2446–2552.
(16) Stein, R. L. *J. Am. Chem. Soc.* **1983**, *105*, 5111–5116.
(17) Stein. R. L. *J. Am. Chem. Soc.* **1985**, *107*, 5767–5775.
(18) Sutton, L. D.; Stout, J. S.; Hosie, L.; Spencer, P. S.; Quinn, D. M. *Biochem. Biophys. Res. Commun.* **1986**, *134*, 386–392.
(19) Rudd, E. A.; Mizuno, N. K.; Brockman, H. L. *Biochim. Biophys. Acta* **1987**, *918*, 106–114.
(20) Smith, P. K.; Krohn, R. I.; Hermanson, G. T.; Mallia, A. K.; Gartner, F. H.; Provenzano, M. D.; Fujimoto, E. K.; Goeke, N. M.; Olson, B. J.; Klenk, D. C. *Anal. Biochem.* **1985**, *150*, 76–85.
(21) Burdette, R. A.; Quinn, D. M. *J. Biol. Chem.* **1987**, *261*, 12016–12021.
(22) Quinn, D. M.; Sutton, L. D.; Kinzelman, T. J. *Am. Biotechnol. Lab.* **1988**, *6*, 33–37.
(23) Salomaa, P.; Schaleger, L. L.; Long, F. A. *J. Am. Chem. Soc.* **1964**, *86*, 1–7.
(24) Schowen, K. B. J. In *Transition States of Biochemical Processes*; Gandour, R. D., Schowen, R. L., Eds.; Plenum Press: New York, 1978; pp 225–283.
(25) Schowen, K. B.; Schowen, R. L. *Methods Enzymol.* **1982**, *87*, 551–606.
(26) Wentworth, W. E. *J. Chem. Educ.* **1965**, *42*, 96–103.

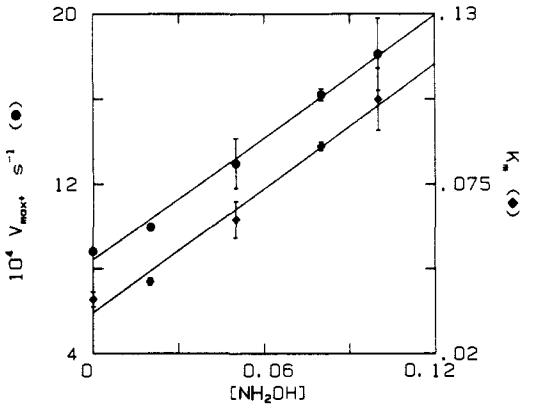

Figure 1. Effect of hydroxylamine on V (closed circles) and K (closed diamonds) of CEase-catalyzed hydrolysis of PNPL. The solid lines are linear least-squares fits. Reactions were followed at 400 nm in 0.1 M sodium phosphate buffer, pH 7.1, that contained 0.1 N NaCl, 1.1 mM TX100, 38 μM PNPL, 1.31 μg mL^{-1} CEase, and the indicated concentrations of NH_2OH. Reaction temperature was 20.4 ± 0.1 °C.

the solvent isotope effect (i.e., $x = 1$), quadratic and downward bulging if two protons contribute (i.e., $x = 2$), etc. The contribution of a transition-state proton to the solvent isotope effect is just the reciprocal of its fractionation factor, $1/\phi^T_i$. The mathematical function that best describes a particular proton inventory was determined by polynomial regression analysis.[27]

A proton inventory that bulges upward suggests a change in rate-determining step[24,25,28,29] and is fit to eq 5.[28,29] C, the commitment to

$$\frac{k_n}{k_1} = \frac{(1 + C\phi^T)(1 - n + n\phi^T)}{\phi^T + C\phi^T(1 - n + n\phi^T)} \quad (5)$$

proton-transfer catalysis, is a measure of rate determination by the solvent isotope sensitive transition state. The commitment will be further discussed later. The rate constant in D_2O is k_1, and the intrinsic solvent isotope effect is $1/\phi^T$.

Results

Nucleophilic Trapping of Lauryl–CEase Intermediate. Stout et al.[9] showed by nucleophilic trapping with short-chain alcohols that V_{max} of CEase-catalyzed hydrolysis of PNPB is rate-limited by deacylation, as described by the mechanism in Scheme II. Addition of nucleophiles activates CEase-catalyzed reactions by providing an alternate pathway for forward flux through the acylenzyme intermediate F. When deacylation is rate-limiting (i.e., $k_3 \gg k_5$, k_7[Nu:]), both V and K depend linearly on [Nu:]:

$$V = (k_5 + k_7[\text{Nu:}])[E_T] \quad (6)$$

$$K = (K_s/k_3)(k_5 + k_7[\text{Nu:}]) \quad (7)$$

V/K, however, is independent of [Nu:]:

$$V/K = (k_3/K_s)[E]_T \qquad K_s = \frac{k_2 + k_3}{k_1} \quad (8)$$

Equation 8 emphasizes that V/K, which monitors microscopic steps that convert free enzyme and free substrate to the acylenzyme intermediate, is always an acylation rate constant.

Figure 1 shows the linear dependences, predicted by eqs 6 and 7, of V and K on NH_2OH concentration for CEase-catalyzed hydrolysis of PNPL. Similar results were obtained when the alternate nucleophiles were $MeONH_2$, NH_2NH_2, ethylenediamine, and imidazole. Therefore, V for CEase-catalyzed hydrolysis of PNPL is rate-limited by deacylation. Moreover, the lauryl-hydroxamate product was quantitated as described by Burdette and Quinn.[21] A 30-mL reaction mixture that contained 38 μM PNPL, 0.1 M NH_2OH, and 1.8 μg/mL of CEase produced 45 μg of laurylhydroxamate, whereas the corresponding control contained 11 μg of the transacylation product. Therefore, lauryl hydroxamate formation is catalyzed by CEase.

A possible complication in the nucleophilic trapping experiments just described is that not all of the enzyme is bound to the micelle surface, and thus, alternate nucleophiles may affect the rate by affecting the fraction of enzyme that is surface-bound. This complication is obviated by the fact that the initial velocity of CEase-catalyzed hydrolysis of PNPL is independent of total micelle concentration over the range 0.27–2.7 mM for mixed TX100 micelles that contain 4 mol % of PNPL.[30] If there were enzyme that was not surface-bound, the rate would increase as micelle concentration increases. Therefore, in the lipid p-nitrophenyl ester assays described herein, CEase is entirely bound to micelles.

Kinetic Parameters for Lipid p-Nitrophenyl Ester Hydrolyses. Table I lists the kinetic constants k_{cat} and k_{cat}/K for the CEase-catalyzed hydrolysis of eight p-nitrophenyl esters. As discussed above, deacylation is rate-limiting for both PNPB and PNPL, and hence, k_{cat} values for all the PNP esters are deacylation rate constants. As Table I shows, the deacylation rates for C_4–C_8 esters are approximately equal, with a slight maximum for PNPC, but the deacylation rate drops off precipitously for the C_{10} and C_{12} esters.

Table I. Kinetic Constants and Solvent Isotope Effects for CEase-Catalyzed Hydrolysis of Lipid p-Nitrophenyl Esters[a]

substrate	z[b]	$10^{-4}k_{cat}/K$, $M^{-1}s^{-1}$	k_{cat}, s^{-1}	$^{D_2O}k_{cat}/K$	$^{D_2O}k_{cat}$
PNPA	2	5.0 ± 0.1	ND[c]	1.81 ± 0.03	ND[c]
PNPP	3	30.3 ± 0.1	ND[c]	2.1 ± 0.1	ND[c]
PNPB	4	37.7 ± 0.1	26.9 ± 0.1	2.00 ± 0.02	2.36 ± 0.07
PNPV	5	74 ± 2	28.5 ± 0.9	1.41 ± 0.03	2.12 ± 0.02
PNPC	6	125 ± 1	33.1 ± 0.1	1.47 ± 0.01	2.01 ± 0.03
PNPO	8	26.3 ± 0.1	22 ± 5	1.27 ± 0.08	2.6 ± 0.5
PNPD	10	5.32 ± 0.01	2.0 ± 0.1	1.24 ± 0.05	1.65 ± 0.07
PNPL	12	1.05 ± 0.01	0.7 ± 0.1	1.21 ± 0.01	2.1 ± 0.5

[a] Reactions were performed as described in the Experimental Section at 25.1 ± 0.4 °C. The kinetic parameters k_{cat} and K were calculated by fitting time course data to eq 1 for reactions in which $[S]_0 > K$, and k_{cat}/K values were determined by fitting time courses to eq 2 for reactions in which $[S]_0 \leq K/10$, as described in the Experimental Section. [b] Number of carbons in the fatty acyl portion of substrate. [c] Not determined because K is greater than the maximum solubility of the substrate.

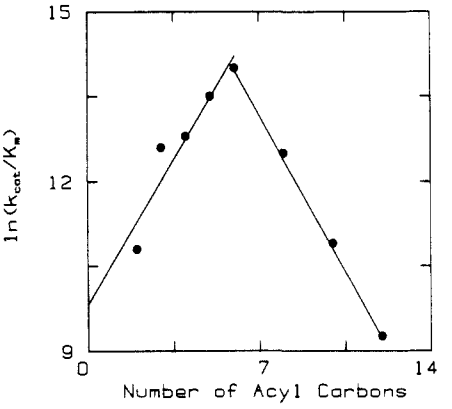

Figure 2. Linear free energy correlations, plotted as ln (k_{cat}/K) versus the number of carbons in the fatty acyl chain of the substrate for CEase-catalyzed hydrolysis of lipid p-nitrophenyl esters. For reaction conditions, see the Experimental Section and footnote a of Table I. The lines are linear least-squares fits, as described in the Results. The equations of the ascending and descending linear fits are, respectively, ln (k_{cat}/K) = (0.73 ± 0.14)z + (9.8 ± 0.6) and ln (k_{cat}/K) = (−0.797 ± 0.005)z + (18.84 ± 0.05).

(27) Polynomial regression analyses were performed with the computer program MYSTAT, a version of the program SYSTAT that is designed to run on a personal computer. The program was purchased from SYSTAT, 1800 Sherman Ave., Evanston, IL 60201.

(28) Quinn, D. M.; Swanson, M. L. *J. Am. Chem. Soc.* **1984**, *106*, 1883–1884.

(29) Acheson, S. A.; Barlow, P. N.; Lee, G. C.; Swanson, M. L.; Quinn, D. M. *J. Am. Chem. Soc.* **1987**, *109*, 246–252.

(30) Stout, J. S.; Quinn, D. M. Unpublished observations.

Scheme III

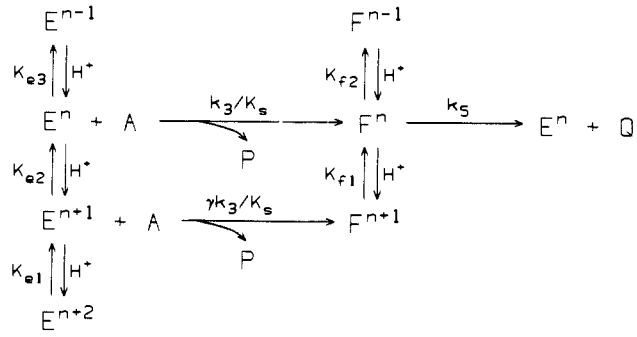

The acylation rate constant rises to a sharp maximum for the C_6 substrate *p*-nitrophenyl caproate, which has $k_{cat}/K = 1.25 \times 10^6$ M^{-1} s^{-1}, as shown in Table I. Figure 2 shows a plot of ln (k_{cat}/K) versus the number of fatty acyl carbons of substrates. Both the ascending and descending limbs of this plot define linear free energy relationships that are described by the following equations:

$$k_{E,0} = \frac{k_B T}{h} e^{-\Delta G^{\ddagger}/RT} \quad (9)$$

$$k_{E,z} = \frac{k_B T}{h} e^{-(\Delta G^{\ddagger} + z\Delta\Delta G^{\ddagger})RT} \quad (10)$$

Equation 9 is the absolute rate theory equation[31] for $k_{E,0}$, which is k_{cat}/K for a hypothetical reaction in which there are no carbons in the fatty acyl chain of the ester. Equation 10 postulates that addition of successive fatty acyl carbons is accompanied by equal and additive contributions to the free energy of activation. Substitution of eq 9 into eq 10 and natural logarithm transformation yields the following linear free energy equation:

$$\ln (k_{E,z}) = \ln (k_{E,0}) - z\Delta\Delta G^{\ddagger}/RT \quad (11)$$

In eqs 10 and 11, z is the number of carbons in the acyl chains of substrates. Linear least-squares analysis of the ascending and descending limbs of Figure 2 gives $\Delta\Delta G^{\ddagger} = -430 \pm 80$ and 472 ± 3 cal/mol per methylene unit, respectively. The increment on the descending limb is about half the per methylene unit free energy dependence described by Tanford[32] for phase transfer of hydrophobic molecules from a hydrocarbon solvent to H_2O. Therefore, substrates in this portion of the plot appear to get wetter on conversion from the free enzyme and free substrate reactant state to the acylation transition state. The increment on the ascending limb is about half what one expects for phase transfer from H_2O to a hydrocarbon solvent and indicates that the substrate gets dryer on conversion of the reactant state to the transition state. There will be more on these observations later.

Solvent Isotope Effects. Table I also contains solvent deuterium isotope effects on k_{cat} and k_{cat}/K. As expected for a serine esterase, all isotope effects are normal. Solvent isotope effects for acylation show a systematic decrease as the chain length of the substrate increases and level off for long substrates at $^{D_2O}k_{cat}/K \approx 1.2$. This trend in solvent isotope effects suggests that the structure of the rate-determining transition state changes as the substrate structure is varied. For the two shortest substrates, PNPA and PNPP, the observed isotope effects are smaller than the intrinsic isotope effects; this matter is addressed below when proton inventory results are presented.

pH-Rate Profiles. The pH-V and pH-V/K profiles for CEase-catalyzed hydrolysis of PNPB are presented in Figure 3, and the appropriate kinetic mechanism is shown in Scheme III. The pK_a values from fitting the pH-V profile to eq 3 are $pK_{f1} = 3.94 \pm 0.07$ and $pK_{f2} = 9.1 \pm 0.1$, and V^{lim} is $9.0 \pm 0.2 \times 10^{-7}$ M s^{-1}. Since the corresponding K_a values are separated by $>10^5$,

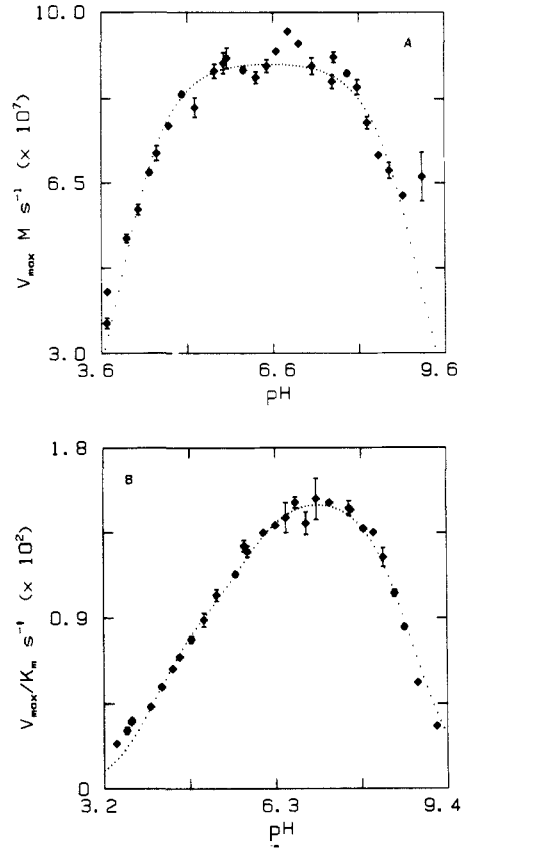

Figure 3. pH-V profile (A) and pH-V/K profile (B) for CEase-catalyzed hydrolysis of PNPB. Reactions were conducted as described in the Experimental Section at 24.8 ± 0.2 °C. The reaction buffers were 0.1 M sodium formate/formic acid (pH 3.25–3.69), 0.1 M sodium acetate/acetic acid (pH 3.70–5.80), 0.1 M NaH_2PO_4/Na_2HPO_4 (pH 5.74–7.64), and 0.1 M trisma/trisma·HCl (pH 7.69–9.20). All buffers contained 0.1 N NaCl, 1 mM TX100, 2% MeCN (v/v), and 300 μM PNPB. CEase concentrations were 12 μg mL^{-1} (pH 3.25–3.70), 8 μg mL^{-1} (pH 4.04–4.44 and 9.20), 4 μg mL^{-1} (pH 4.78–6.09 and 8.08–8.86), and 2 μg mL^{-1} (pH 6.31–7.90).

a broad plateau of maximal activity is observed.

For the pH-V/K profile of Figure 3B, the basic pK_a was calculated by fitting data at pH ≥ 7 to eq 12. The calculated

$$V/K^{obs} = \frac{V/K^{lim}}{1 + 10^{pH-pK_{e3}}} \quad (12)$$

values are $pK_{e3} = 8.7 \pm 0.1$ and $V/K^{lim} = 1.56 \pm 0.03 \times 10^{-2}$ s^{-1}. The pK_a value agrees well with that calculated for the basic limb of the pH-V profile. The activity on the acid limb of the pH-V/K profile is not governed by a single pK_a. Therefore, the profile was modeled by putting the parameters calculated above for the basic limb into eq 13 and entering guesses for the other constants until

$$V/K = \frac{V/K^{lim}(1 + \gamma 10^{pK_{e2}-pH})}{1 + 10^{pK_{e1}+pK_{e2}-2pH} + 10^{pK_{e2}-pH} + 10^{pH-pK_{e3}}} \quad (13)$$

the fit was visually satisfying. This procedure was used to generate the theoretical fit shown in Figure 3B. In eq 13, pK_{e1} and pK_{e2} are successive pK_a values on the acidic limb of the profile and γ is the fraction of maximal activity of the E^{n+1} form of the enzyme shown in Scheme III. The values used to generate the fit of Figure 3B are $pK_{e1} = 4.1$, $pK_{e2} = 5.8$, and $\gamma = 0.58$. Though these values are not uniquely determined, $pK_{e1} = 4.1$ agrees well with $pK_{f1} = 3.94 \pm 0.07$ from the pH-V profile.

Proton Inventories. Figure 4 shows linear proton inventories for V of CEase-catalyzed hydrolysis of PNPB and PNPD, and therefore, the observed solvent isotope effects arise from single proton transfers in the deacylation transition state. Linear proton inventories for V were also observed for PNPV, PNPC, PNPO, and PNPL. Two methods of analysis support a linear model.

(31) Glasstone, S.; Laidler, K. J.; Eyring, H. *The Theory of Rate Processes*; McGraw-Hill: New York, 1941.

(32) Tanford, C. *The Hydrophobic Effect: Formation of Micelles and Biological Membranes*; Wiley: New York, 1980; pp 5–13.

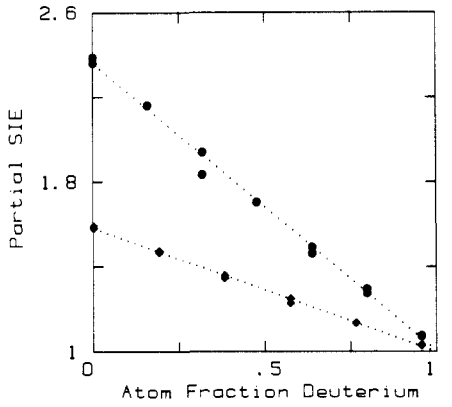

Figure 4. Proton inventories for V of CEase-catalyzed hydrolysis of PNPB (closed circles) and PNPD (closed diamonds). Reactions were performed at 24.98 ± 0.02 and 25.32 ± 0.02 °C, respectively, under conditions described in the Experimental Section. Theoretical fits to eq 4 are represented by the dotted lines. In addition to 1 mM TX100, reactions contained 400 μM PNPB and 26 μg mL^{-1} CEase or 50 μM PNPD and 40 μg mL^{-1} CEase.

Table II. Reaction Dynamics and Intrinsic Isotope Effects for the Acylation Stages of CEase-Catalyzed Hydrolysis of PNPA and PNPP

substrate	$^{D_2O}k_5$[a]	C[a]	f_3[b]	f_5[b]
PNPA	2.12 ± 0.05	0.5 ± 0.2	0.33 ± 0.14	0.67 ± 0.14
PNPP	2.9 ± 0.1	0.7 ± 0.1	0.41 ± 0.06	0.59 ± 0.06

[a] C and $^{D_2O}k_5$ are the commitment to catalysis and the intrinsic solvent isotope effect, respectively, and were determined by fitting V/K proton inventories to eq 5, as discussed in the text. Error limits are standard errors of the least-squares fit.[26] [b] The values of f_3 and f_5 are fractions of rate determination by the isotopically insensitive and the isotopically sensitive transition states, respectively, and are calculated as follows:[36] $f_3 = C/(1 + C)$ and $f_5 = 1/(1 + C)$.

Polynomial regression analyses show that the linear term only is highly significant for all of the proton inventories. When the quadratic term is significant (e.g., for PNPB the quadratic term was significant at the 90% confidence level), nonlinear least-squares fitting of the proton inventory to the quadratic version of eq 4 shows that the isotope effect comes predominantly from a single transition-state fractionation factor. Therefore, the analyses of V proton inventories, taken en masse, support a deacylation transition state that is stabilized by simple general-acid–base catalysis.

The V/K proton inventories fall into three groups: (a) For PNPA and PNPP, the two shortest substrates, the proton inventories are nonlinear and bulge upward, as Figure 5 shows for PNPA. This behavior is consistent with a model in which both isotopically sensitive and insensitive microscopic transition states contribute to rate determination. The results of nonlinear least-squares fitting to eq 5 of the V/K proton inventories for PNPA and PNPP are given in Table II. (b) For PNPB, the observed isotope effect is sizable ($^{D_2O}V/K = {}^{D_2O}k_{cat}/K = 2.00$) and the proton inventory is linear. Therefore, the acylation transition state for PNPB is stabilized by simple general-acid–base catalysis. (c) For the longer substrates PNPV through PNPL, $^{D_2O}V/K$ is <1.5 and the proton inventories are apparently linear (see plots for PNPC and PNPD in Figure 5). However, especially for PNPO through PNPD for which $^{D_2O}V/K$ is ~1.2, it is not wise to rationalize the diminutive isotope effects in terms of transition-state proton transfer. Rather, some physical process must be increasingly rate-limiting as the fatty acyl chain length increases.

Discussion

The results described in this paper provide a seminal view of some of the features of the molecular dynamics of CEase catalysis. The kinetic and chemical trapping of the lauryl–CEase intermediate by alternate nucleophiles demonstrate that, as for short substrates, k_{cat} for substrates that have long acyl chains is rate-limited by turnover of acylenzyme intermediates. Stout et al.[9] came to a similar conclusion for nucleophilic trapping by short-chain alcohols of the butyrylenzyme intermediate in porcine and bovine pancreatic CEase-catalyzed turnover of PNPB, and Lombardo and Guy[33] proposed an acylenzyme mechanism for human pancreatic CEase-catalyzed hydrolysis of PNPA, propyl thioacetate, triacetin, and methyl butyrate. Even though lipid p-nitrophenyl esters are somewhat distant structurally from the physiological substrates of the enzyme, the deacylation stage of the catalytic mechanism is identical with that of physiological CEase catalysis. This assertion is supported by the fact that k_{cat} values for p-nitrophenyl decanoate (cf. Table I) and for the sn-1 thioester analogue of didecanoylphosphatidylcholine are similar;[34] since both substrates produce the same decanoyl–CEase intermediate, the similarity of k_{cat} values indicates that deacylation is rate-determining for both. Furthermore, the trend in k_{cat} values with increasing fatty acyl chain length defines the structural dependence of the lifetime of acylenzyme intermediates. The C_4–C_8 acylenzymes turn over rapidly, whereas that of the C_{10} and C_{12} acylenzymes drops precipitously. Despite this sensitivity of rate to acylenzyme structure, the deacylation transition states for all substrates are stabilized by single proton transfers that generate solvent isotope effects of $^{D_2O}V \approx 2$. Therefore, unlike serine protease reactions,[13-17] proton inventories of the deacylation stage of the CEase mechanism provide no indication of charge-relay catalysis or of other multiproton contributions to transition-state stabilization.

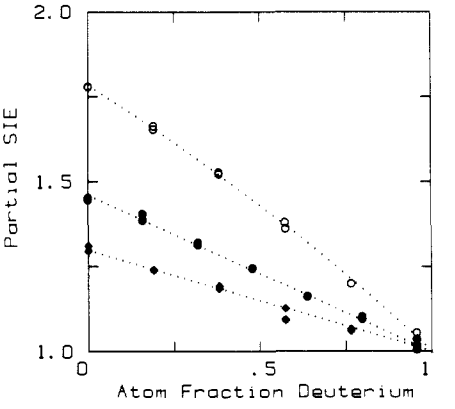

Figure 5. Proton inventories for V/K of CEase-catalyzed hydrolysis of PNPA (open circles), PNPC (closed circles), and PNPD (closed diamonds). Reactions were conducted at 25.31 ± 0.02 °C under conditions described in the Experimental Section. Theoretical fits, represented by dotted lies, are to eq 4 for PNPC and PNPD and to eq 5 for PNPA. In addition to 1 mM TX100, reactions contained 40 μM PNPA and 186 μg mL^{-1} CEase, 50 μM PNPC and 3.2 μg mL^{-1} CEase, or 50 μM PNPD and 40 μg mL^{-1} CEase.

Solvent isotope effects on V and proton inventories were determined at pL (L = H, D) values that are in the flat crest of the pH–V profile (cf. Figure 3), while those on V/K were determined at the maximum of the pH–V/K profile. Therefore, the solvent isotope effects on ionizations of amino acid side chains in the free enzyme or the acylenzyme intermediate do not complicate interpretation of the proton inventories. The pH–V profile yielded butyryl-CEase ionization constants of $pK_{f1} = 3.94$ and $pK_{f2} = 9.1$. The acidic pK_a value may indicate that V depends on the basic form of an aspartic or glutamic acid side chain.[35] The sequence similarity of active-site regions of CEase,[10] AChE,[11] and BuChE[12] suggests that an active-site histidine functions in the CEase mechanism as a general-acid–base catalyst, a long-known feature of cholinesterase catalysis.[36] Lombardo[35] modified nine histidines of human pancreatic CEase with ethoxyformic anhydride, only

(33) Lombardo, D.; Guy, O. *Biochim. Biophys. Acta* **1981**, *657*, 425–437.
(34) The k_{cat} value for CEase-catalyzed hydrolysis of didecanoyl-*rac*-1-thioglycerophosphocholine, 0.7 s^{-1}, is similar to that for p-nitrophenyl decanoate, 2.0 s^{-1}. Therefore, turnover of the phospholipid must be prominently rate-limited by deacylation.
(35) Lombardo, D. *Biochim. Biophys. Acta* **1982**, *700*, 67–74.
(36) Quinn, D. M. *Chem. Rev.* **1987**, *87*, 955–979.

one of which is required for activity, and suggested that the essential histidine is the residue that has a pK_a of 6.9 on which substrate hydrolysis activity depends.[37] We find no such pK_a on the acidic limbs of either the pH–V or pH–V/K profiles. It is possible that the pK_a of the active-site histidine is suppressed in the butyryl-CEase intermediate and that the pK_a of 5.8 estimated from the pH–V/K profile is that of an active-site histidine. Though the cumulative circumstantial evidence for a CEase active-site histidine is substantial, it is premature at this point to make such an assignment. This question of the identity of active-site amino acids (other than Ser-194) can be addressed by determining pH–rate profiles for native CEase and for CEase structural variants that are produced by site-directed mutagenesis.

The structure–reactivity behavior of V/K and its corresponding interpretation in terms of acylation transition-state structure are considerably more complex than the picture outlined earlier for deacylation. There is a progressive decrease in solvent isotope effects (cf. Table I) and a bipartite linear free energy plot (cf. Figure 2) as the fatty acyl chain length of the substrate increases. These observations suggest that a change either in reaction pathway (parallel transition states) or in rate-determining step (serial transition states) is occurring. Of these possibilities, that involving parallel reaction pathways is favored for two reasons: (a) The slope of the linear free energy plot for the C_2–C_6 substrates is −430 cal/mol per methylene unit, which indicates that the substrate is partitioning from an aqueous to a more lipidic environment on conversion of the reactants (free substrate and micelle-bound free enzyme) to the acylation transition state. The shorter substrates have sufficient water solubility that TX100 micelles are not required for their dissolution, and thus, it is reasonable to suggest that the free substrate is predominantly in the aqueous phase. (b) The slope of the linear free energy plot for the C_6–C_{12} substrates is 470 cal/mol per methylene unit, nearly the same magnitude as but opposite in sign to that for the shorter substrates. Therefore, the longer substrates experience a change from a more lipidic to a less lipidic (more aqueous) environment on conversion of the reactants to the transition state. Because of the sparing water solubility of the longer lipid *p*-nitrophenyl esters,[38] it is reasonable to suggest that the free substrate of the reactant state is predominantly associated with TX100 micelles. It is interesting that the difference in the slopes for the long and short substrates is 900 ± 90 cal/mol per methylene unit, which is identical within error to free energies of transfer from hydrocarbon solvents to water of homolous alkanes and functionalized alkanes.[32] This is to be expected if short and long lipid *p*-nitrophenyl esters bind to the same site on CEase, since the difference in slopes would then represent the free energy of transfer, per methylene unit, from the micelle to the aqueous phase.

The progressive decrease in observed solvent isotope effect as substrate fatty acyl chain length increases suggests that the intrinsic solvent isotope effect for V/K of long-chain substrates is very small. For the C_8, C_{10}, and C_{12} substrates, the isotope effects are ~1.2, which supports this idea. Therefore, for the long substrates residing primarily in mixed micelles with TX100, the chemical transition state does not contribute appreciably to acylation rate determination. It is tempting to propose that the energetic cost of extraction of the substrate into the CEase active site is sufficiently high that substrate binding, a physical step, controls the rate. This process is not expected to generate much of a solvent isotope effect and is in accord with the slope of the decending limb of the free energy plot of Figure 2.

The two shortest substrates, PNPA and PNPP, fall on the bottom of the ascending limb of the free energy plot of Figure 2 and have proton inventories of V/K that bulge upward. Therefore, for these substrates, serial microscopic transition states contribute to rate determination. A kinetic mechanism that can explain the proton inventories for PNPA and PNPP is the following:

$$E + A \underset{k_2}{\overset{k_1}{\rightleftharpoons}} EA_1 \underset{k_4}{\overset{k_3}{\rightleftharpoons}} EA_2 \xrightarrow{k_5} F + P$$

A reversible isomerization interconverts the Michaelis complexes EA_1 and EA_2 and precedes the chemical catalytic step k_5. V/K for this mechanism is given by eq 14. Since the V/K proton

$$V/K = \frac{k_1k_3k_5[E]_T}{k_2(k_4 + k_5) + k_3k_5} \tag{14}$$

inventory for PNPB and the V proton inventories for all substrates are linear, it is reasonable to suggest that the transition state of the k_5 step is stabilized by a single proton transfer and, therefore, the following form of eq 4 applies:

$$k_{5,n} = k_{5,0}(1 - n + n\phi^T_5) \tag{15}$$

In this equation, $k_{5,n}$ and $k_{5,0}$ are the microscopic rate constants in isotopic solvent mixtures and in H_2O, respectively, and the intrinsic isotope effect is ${}^{D_2O}k_5 = 1/\phi^T_5$. Equations 14 and 15 can be used to derive an expression of the form of eq 5,[28,29] in which $C = k_5/k_4$ is the commitment to proton-transfer catalysis. The derivation assumes that the serial transition states of the k_3 and k_5 steps contribute to acylation rate determination and that only the k_5 step produces a solvent isotope effect. The order of isotopically insensitive and sensitive steps is not unique; however, the salient feature of the model, that serial transition states contribute to rate determination, is. The intrinsic solvent isotope effects and commitments determined from the PNPA and PNPP proton inventories are gathered in Table II. The commitments are 0.5 for PNPA and 0.7 for PNPP, which correspond to isotopically insensitive k_3 steps that are 33% and 41% rate-determining, respectively. Therefore, the acylation stages of CEase-catalyzed hydrolysis of these two substrates are rate-determined by virtual transition states,[28,29,36,39-41] and correspondingly the measured isotope effects for V/K underestimate the intrinsic isotope effects for the chemical step. The next paper in this issue describes experiments that further support and describe this virtual transition-state model of CEase acylation reaction dynamics.

Acknowledgment. This work was supported by NIH Grant HL30089 and by a Research Career Development Award to D.M.Q. from the National Heart, Lung and Blood Institute of NIH (HL01583, 1985–1990).

(37) Lombardo, D.; Deprez, P.; Guy, O. *Biochimie* **1980**, *62*, 427–432.

(38) The solubility in our hands of PNPB is ~0.5 mM. Moreover, the free energy of dissolution is less favorable by ~825 cal/mol per methylene unit,[32] which corresponds to ~6-fold-reduced solubility. Therefore, the solubilities of PNPC, PNPO, PNPD, and PNPL are approximately 14 μM, 0.4 μM, 10 nM, and 0.3 nM, respectively. Since the lipid *p*-nitrophenyl ester reactions described herein typically contain ~50 μM substrate, it is obvious that for the longer esters essentially all of the substrate is contained in mixed micelles with TX100.

(39) Stein, R. L. *J. Org. Chem.* **1981**, *46*, 3328–3330.

(40) Schowen, R. L. In *Transition State of Biochemical Processes*; Gandour, R. D., Schowen, R. L., Eds.; Plenum Press: New York, 1978; pp 77–114.

(41) (a) Stein, R. L. *J. Am. Chem. Soc.* **1985**, *107*, 6039–6042. (b) Stein, R. L. *J. Am. Chem. Soc.* **1985**, *107*, 7768–7769. (c) Stein, R. L.; Strimpler, A. M.; Hori, H.; Powers, J. C. *Biochemistry* **1987**, *26*, 1305–1314.